

# Electron temperature measurement of high- $\beta$ plasma in the Ring Trap 1 device

## 磁気圏型プラズマ閉じ込め装置 RT-1 における高 $\beta$ プラズマの電子温度計測

Toahiki Mushiake, Zensho Yoshida, Masaki Nishiura, Haruhiko saito, Yoshihisa Yano, Yohei Kawazura, Miyuri Yamasaki, Ankur Kashyap

虫明敏生, 吉田善章, 西浦正樹, 齋藤晴彦, 矢野善久, 川面洋平, 山崎美由梨, アンクル・カシャーパ

Department of Advanced Energy, Graduate School of Frontier Science, The University of Tokyo  
5-1-5 Kashiwanoha, Kashiwa, Chiba 277-8561, Japan  
東京大学大学院 〒277-8561 柏市柏の葉 5-1-5

The magnetosphere device RT-1 (Ring Trap 1) generates the dipole magnetic field by using a levitated superconducting coil. Gas pressure dependence of the electron temperature was evaluated by detecting soft X-ray emitted from high- $\beta$  plasma. As a result, there are two types of electron temperature, then electron temperature of low and high energy exist in 0.3~0.8 keV and 10~40 keV respectively. Intensity variation of characteristic X-rays emitted from impurities was also estimated.

### 1. Introduction

The magnetosphere device RT-1 (Ring Trap 1) simulates a magnetospheric configuration like that of Jupiter by a dipole magnetic field magnet [1,2]. RT-1, which is expected to be used as an advanced nuclear fusion device, confines high- $\beta$  plasma in the dipole magnetic field.

It is known that high- $\beta$  plasma is confined in magnetosphere like that of Jupiter [1,2]. This is considered due to the influence of diamagnetic effect by dynamic pressure of strong rotation flow. In recent researches, the local electron  $\beta_e$  was found to exceed 1 by electron cyclotron heating (ECH). Currently,  $\beta_e$  is estimated by the equilibrium analysis based on Grad-Shafranov equation. It is essential to measure electron density and temperature distribution because electron energy distribution doesn't necessarily follow Maxwell distribution. The detected soft X-rays were used to determine electron energy distribution in high- $\beta$  plasma.

### 2. Electron temperature measurement

Fig 1 shows the cross sectional view of the RT-1 device.

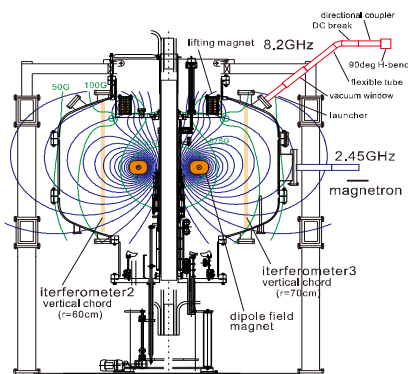


Fig. 1 the cross sectional view of the RT-1 device

### 2.1 Electron energy distribution by Si(Li) detector

In RT-1 Si(Li) detector (AMPTEK XR100) is implemented to detect a soft X-ray spectrum. The detected signal is transmitted to an amplifier for pulse height analysis (PHA). The Si(Li) detector is attached onto the upper port with a Be window for vacuum sealing (thickness:12.7 $\mu$ m) and Pb collimeter (diameter : 8mm) as shown in Fig1.

When analyzing soft X-ray spectra obtained by the Si(Li) detector, the quantum efficiency of the detector and the transmittance of the Be window were taken into account. Fig2 shows corrected soft X-ray spectra from Si(Li) detector [3].

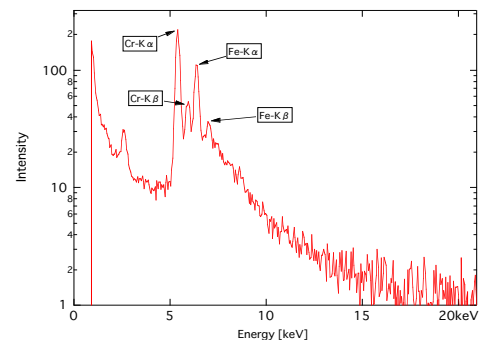


Fig. 2 Soft X-ray spectra (after correction)

The characteristic X-rays of impurities (Fe and Cr) generated by electrons colliding to vacuum furnace wall and internal structures was observed at 5.39keV for Cr-K $\alpha$ , 5.95keV for Cr-K $\beta$ , 6.41keV for Fe-K $\alpha$ , 7.02keV for Fe-K $\beta$ .

### 2.2 Temperature measurement for low and high energy electrons

Electron temperature can be estimated from soft X-ray spectra mainly generated by bremsstrahlung in plasma [4]. When velocity

distribution function of electron follows Maxwell distribution, the intensity of the X-ray spectra is in proportion to

$$n_e n_i Z_{eff}^2 \frac{\exp\left(-\frac{E_x}{T_e}\right)}{E_x \sqrt{T_e}}$$

$n_e$ : electron density  $n_i$ : ion density  $Z_{eff}$ : effective nuclear charge  $E_x$ : photon energy  $T_e$ : electron temperature

Electron temperature was estimated by fitting the corrected spectra [4,5]. Fig3 shows the electron temperatures for high energy component ( $T_{eh}$ ) and low energy one ( $T_e$ ) generated by ECH.

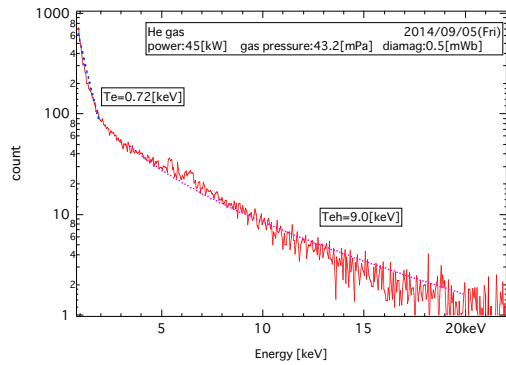


Fig. 3 Raw X-ray spectra and fitting curves of high energy part ( $T_{eh}$ ) and low energy part ( $T_e$ )

$T_{eh}$  and  $T_e$  are 9.0 keV and 0.81 eV from Fig. 3, respectively.

Fig. 4 shows the ECH power dependence of the electron temperature under the constant gas pressure (4.3mPa)

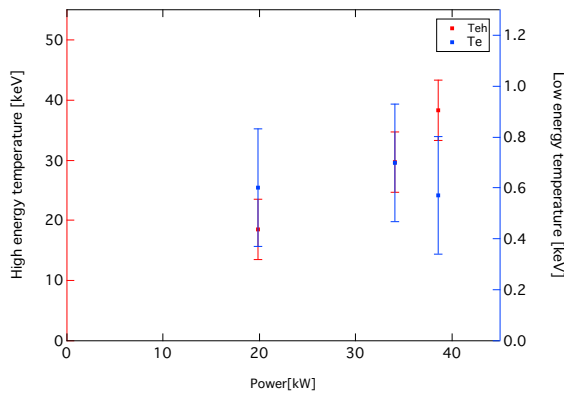


Fig. 4 Power dependence of the electron temperature of low and high energy

It was observed that the electron temperature of high energy component increased as the ECH power was increased. However, the low energy component had no obvious change in this operation region. It is indicated that the ECH power was being absorbed by high energy electrons rather than bulk electrons.

Fig. 5 shows the gas pressure dependence of electron temperature under the constant ECH power (44kW).

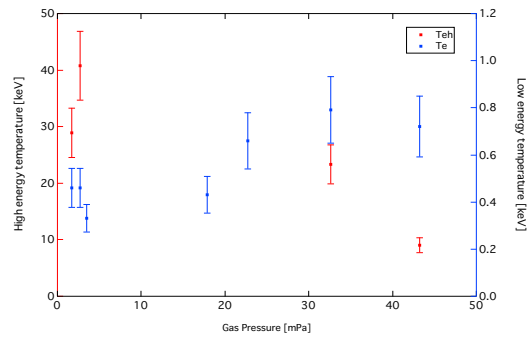


Fig. 5 Gas pressure dependence of the electron temperature of low and high energy

It was observed that the high energy temperature decreased as gas pressure increased and the low energy temperature didn't seem to change from 20mPa to 40mPa.

Fig. 6 shows characteristic X-rays profile detected from impurities.

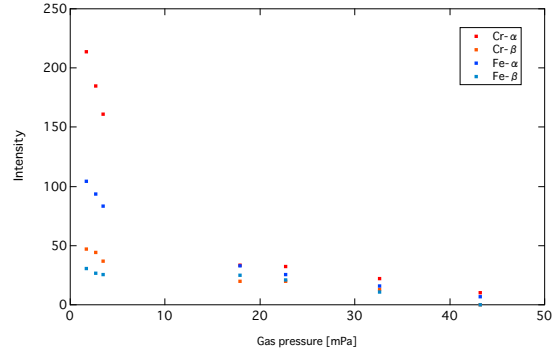


Fig. 6 Gas dependence of characteristic X-ray emitted from impurities

Intensity of the characteristic X-rays emitted from impurities decreased as gas pressure increased from Fig. 6.

### 3. Summary

Electron temperature of low and high energy was estimated. Moreover, power and gas dependence of them was confirmed. In addition, it was also determined what emitted characteristic X-rays.

### Acknowledgments

This work was supported by JSPS KAKENHI Grant Numbers 23224014 and 24360384.

### References

- [1] Z. Yoshida, H. Saitoh, Y. Yano, H. Mikami, W. Sakamoto, J. Morikawa, M. Furukawa, Plasma Physics and Controlled Fusion, 55 (01408), 2013.
- [2] A. C. Boxer, R. Bergmann, J. L. Ellsworth, D. T. Garnier, J. Kesner, M. E. Mauel, and P. Woskov, Nature (London), Phys. Sci. 6, 207 (2010).
- [3] Amptek, Inc.
- [4] I.H. Hutchinson. Principles of Plasma Diagnostics. Cambridge University Press, 1987
- [5] J.E. Rice and K.L. and Chamberlain. X-ray observations between 10 and 150 keV from the Alcator-C tokamak. Physical Review A, 38(3):1461-67, 1988